Available online at www.sciencedirect.com
SCIENCE DIRECT®
Journal of Power Sources 140 (2005) 50–58
JOURNAL OF POWER SOURCES
www.elsevier.com/locate/jpowsour

Direct ethanol fuel cells based on PtSn anodes: the effect of Sn content on the fuel cell performance

W.J. Zhou[a], S.Q. Song[a], W.Z. Li[a], Z.H. Zhou[a], G.Q. Sun[a], Q. Xin[a,b,*], S. Douvartzides[c], P. Tsiakaras[c,**]

[a] *Direct alcohol fuel cell lab, Dalian Institute of Chemical Physics, CAS, P.O. Box 110, Dalian 116023, China*
[b] *State key lab of catalysis, Dalian Institute of Chemical Physics, CAS, P.O. Box 110, Dalian 116023, China*
[c] *Department of Mechanical and Industrial Engineering, School of Engineering, University of Thessaly, Pedion Areos, 38334 Volos, Greece*

Received 29 March 2004; received in revised form 17 July 2004; accepted 16 August 2004
Available online 28 October 2004

Abstract

In the present work, several carbon supported PtSn catalysts with different Pt/Sn atomic ratios were synthesized and characterized by X-ray diffraction (XRD), Transmission electron microscopy (TEM) and X-ray photoelectron spectroscopy (XPS). Both the results of TEM and XRD showed that all in-house prepared carbon supported Pt and PtSn catalysts had nanosized particles with narrow size distribution. According to the primary analysis of XPS results, it was confirmed that the main part of Pt of the as-prepared catalysts is in metallic state while the main part of Sn is in oxidized state. The performances of single direct ethanol fuel cells were different from each other with different anode catalysts and at different temperatures. It was found that, the single DEFC employing Pt_3Sn_2/C showed better performance at 60 °C while the direct ethanol fuel cells with Pt_2Sn_1/C and Pt_3Sn_2/C exhibited similar performances at 75 °C. Furthermore, at 90 °C, Pt_2Sn_1/C was identified as a more suitable anode catalyst for direct ethanol fuel cells in terms of the fuel cell maximum power density. Surface oxygen-containing species, lattice parameters and ohmic effects, which are related to the Sn content, are thought as the main factors influencing the catalyst activity and consequently the performance of single direct ethanol fuel cells.

Keywords: Direct ethanol fuel cells; PtSn/C anode catalysts

1. Introduction

Since 1990s, the large potential market for fuel cell vehicles, portable electrical devices and stationary applications has generated an accelerating interest in polymer electrolyte membrane fuel cells (PEMFCs) directly fed by liquid fuels and operated at lower temperatures. Operating on liquid fuels would eliminate the need for any fuel reformer and greatly simplify the fuel cell system, and therefore, it would assist the rapid introduction of fuel cell technology into commercial markets. Low molecular weight alcohols, methanol and ethanol, are reasonably inexpensive and largely available, having higher electrochemical reactivity at relatively low temperatures. The direct methanol fuel cell (DMFC) technology has already been demonstrated by Ballard [1], the Los Alamos National Laboratory [2] and others [3–6] to possess many beneficial characteristics appropriate to the commercial application, and great progresses have been made in this field recently [7–8]. The oxidation of methanol over Pt alloyed with other metals has been accepted as a method to overcome the insufficient activity of pure Pt for these purposes. Pt alloying for methanol oxidation intends to the establishment of a bi-functional catalytic system that must be capable of both chemisorbing methanol on Pt sites and promoting oxidation of the chemisorbed CO

* Corresponding author. Tel.: +86 411 84379071; fax: +86 411 84379071.
** Co-corresponding author. Tel.: +30 24210 74065.
E-mail addresses: xinqin@dicp.ac.cn (Q. Xin), tsiak@mie.uth.gr (P. Tsiakaras).

0378-7753/$ – see front matter © 2004 Elsevier B.V. All rights reserved.
doi:10.1016/j.jpowsour.2004.08.003

fragment by the secondary metal addition. These studies of Pt alloyed with other noble metals have shown that Ru has by far the largest promoting effect and the bi-functional mechanism of oxidation in PtRu catalysts has been a subject of detailed experimental investigation over the last 20 years [9–14].

In order to extend the practical application of low-temperature fuel cells and facilitate their penetration into the transport market it is also desirable to increase the number of liquid fuels that can be employed in these devices. As an alternative to methanol, ethanol is safer, non-toxic, more convenient, and has greater energy density (8.01 kWh kg^{-1} versus 6.09 kWh kg^{-1}). In addition, ethanol can be easily produced in great quantity through fermentation of sugar-containing raw materials. Therefore, it is more attractive and appears to fulfill most of the requirements of the fuel for low-temperature fuel cells. Thus, besides DMFC, direct ethanol fuel cell (DEFC) is another promising low-temperature fuel cell [13–16].

Compared to DMFC, the present development of DEFC is still not satisfying although ethanol electro-oxidation has been investigated for over 20 years [17]. At present, the main obstacles facing DEFC development are the slow anode kinetics, the catalyst poisoning brought about by the CO-like intermediates at low temperatures and the reactants short circuit. The complete ethanol anodic oxidation, oxygen reduction and overall reaction of DEFC could be described as follows:

Anode reaction:

$$CH_3CH_2OH + 3H_2O \rightarrow 2CO_2 + 12H^+ + 12e^-,$$

$$E^- = 0.084\,\text{V versus SHE}$$

Cathode reaction:

$$3O_2 + 12H^+ + 12e^- \rightarrow 6H_2O,$$

$$E^+ = 1.229\,\text{V versus SHE}$$

Overall reaction:

$$CH_3CH_2OH + 3O_2 \rightarrow 2CO_2 + 3H_2O, \quad E_{emf} = 1.145\,\text{V}$$

Here, E^- and E^+ denote the anodic and cathodic reaction potentials, respectively and E_{emf} denotes the standard electromotive force ($E^+ - E^-$). SHE denotes the standard hydrogen electrode.

It is noticed that the complete electro-oxidation of ethanol involves the release of 12 electrons per ethanol molecule and the cleavage of the C–C bond. The latter is believed to play a key role in the ethanol electro-oxidation and has a determining effect on the fuel cell efficiency and the electrical energy yield. Besides the cleavage of the C–C bond, the CO-like intermediate fragments, which are formed during the dissociative adsorption of ethanol on the catalyst sites, need an oxidative removal [17]. Both these requirements render the electro-oxidation of ethanol more complicated than that of methanol and impose the necessity for more active and selective anode catalysts. In this case, the addition of Ru to Pt was found in many cases to decrease its electrocatalytic activity towards ethanol oxidation, owing to the inactivity of Ru towards the adsorption of ethanol and the cleavage of the C–C bond [18]. On the contrary, other bimetallic and trimetallic electrocatalysts such as PtSn and PtRuSn have been investigated toward ethanol electro-oxidation and exhibit better activity than pure Pt and PtRu catalysts [16,18].

The present investigation has been undertaken the effort to examine in detail the effect of Sn content in the PtSn alloy catalysts. Following the previous work [19], several carbon supported PtSn catalysts with different Pt/Sn atomic ratio were synthesized using a novel preparation method and then employed as anode catalysts for direct ethanol fuel cells operating at different temperatures. Transmission electron microscopy (TEM), X-ray powder diffraction (XRD) and X-ray photoelectron spectroscopy (XPS) were employed as catalyst characterization techniques.

2. Experimental

All carbon (Vulcan XC-72R, Cabot Co., S_{BET} = 237 m^2/g) supported Pt and PtSn catalysts were synthesized as follows [19]. An ethylene glycol solution containing precursors of Pt and Sn was mixed with carbon slurry, and kept at 120 °C for 1 h after pH was adjusted to 13. The reduced mixtures were then acidified again at room temperature. The reduced metals supported on carbon were filtered and washed with copious distilled water. The in-house catalysts were obtained after the filter cake was dried in vacuum oven at 70 °C for 12 h. All catalysts were marked as Pt_xSn_y (subscript denotes the atomic ratio). The Pt content in each sample was 20 wt.%. XRD analysis was carried out to obtain all reflection peaks. Pt(2 2 0) reflection peak was scanned finely again and was fitted using the Gaussian function to calculate the particle size and lattice parameters [20]. The nanoparticle sizes of different Pt-based catalysts were also investigated by TEM. More than 300 particles were calculated to obtain the integrated information of each catalyst. X-ray photoelectron spectroscopy characterization of catalysts was performed on a VG ESCA LABMKII X-ray photoelectron spectrograph under a vacuum of 10^{-9} Pa. Mg Kα ray was used as excitation source ($h\nu$ = 1253.6 eV). C_{1s} was used as the internal standard to calibrate the binding energy results. The membrane electrode assemblies (MEAs), in which the cathode was commercial Pt/C catalyst (20 wt.%) with a metal loading of 1.0 mg Pt/cm^2, were fabricated by pressing the electrodes onto both sides of Nafion®-115 membranes at 130 °C for 90 s [21]. The anode included the different in-house carbon-supported PtSn catalysts with a Pt loading of 1.3 mg/cm^2 (except that the metal loading was 2.0 mg/cm^2 when Pt/C was used as anode catalyst). The MEAs were fastened between two stainless steel polar plates with a dotted flow field and fixed on an in-house single-cell test apparatus. Two aureate

wire nettings were placed between the bipolar plates and the MEAs to collect current. In the DEFCs, unhumidified oxygen with 2 atm (abs.) backpressure was directly fed to the cathode side and 1.0 mol/L of ethanol solution without backpressure at a flow rate of 1.0 mL/min was directly fed to the anode side. Every single cell has been operated for at least three days. On the first day, the single cell was fed only by distilled water to the anode at 75 °C for at least 4 h in order to fully hydrate the electrolyte membrane in the MEAs and remove any low molecular weight organic impurity on the anode firstly. Then the anode was fed by aqueous solution of ethanol. The cell voltage–current density data were collected on the second day. The power density–current density data were obtained from the multiplication of the cell voltage and the corresponding current density. The anode polarization tests of ethanol electro-oxidation over PtSn catalysts were conducted by employing a Potentiostat/Galvanostat Model 273A (EG&G) under the condition of the single fuel cell at 90 °C, in which cathode was fed directly not by oxygen but with the humidified hydrogen and served both as counter electrode and as reference electrode.

3. Results and discussion

3.1. XRD and TEM results

There were no obvious peaks for Sn or its oxides in the XRD patterns of all PtSn catalysts. During our experiments no special XRD peaks for Sn or its oxides were found even after the PtSn catalysts, which were synthesized by employing a novel method, were treated at high temperatures. XRD patterns of all Pt-based catalyst samples clearly and only demonstrated the characteristic peaks of the Pt fcc structure. It was also found from the XRD patterns that there was an obvious 2θ shift to lower angle for PtSn catalysts, which became more obvious as the Sn content increased. The 2θ of the Pt(2 2 0) peak for PtSn with different atomic ratio has angle shift lower than that for Pt as it is summarized in Table 1. The lower angle shift of the Pt peaks and the absence of XRD peaks for Sn and its oxides account for the alloy formation and the interaction between Pt and Sn. Average particle size and fcc lattice parameters for single-phase Pt-based catalysts were evaluated according to the full width at half-maximum (FWHM) and the angular position of the Gaussian-fitted (2 2 0) peaks, respectively. Table 1 clearly shows that the addition of Sn to the Pt extends the fcc lattice parameters and that the lattice parameters of the PtSn catalyst increase as the Sn content increases in comparison with that of pure Pt, indicating the interaction between Pt and Sn [22,23].

As observed from a typical TEM patterns shown in Fig. 1 , most of metal particle sizes of each sample are less than 6 nm, and the nanoparticles show homogeneous dispersion with similar particle sizes. Most of particles are in spherical shape, and no agglomerations are observed. The particle size is approximately 1.5–3.5 nm with a very sharp size distribution, which is in good agreement with the XRD results. Finally, XRD and TEM results jointly indicate (Table 1) that the catalysts investigated here have similar mean nanoparticle sizes (1.5–3.5 nm) with homogeneous dispersion, demonstrating the suitability of the method to prepare nanometer catalysts with a high metal loading.

3.2. XPS results

In Fig. 2, are reported the Sn 3d (a) and Pt 4f (b) spectra for Pt/C, Pt_3Sn_2/C and Pt_1Sn_1/C catalysts. Limited to our present analysis conditions, all the spectra have not been exactly deconvoluted into different components. The binding energies of the elemental Pt and Sn in various catalysts as obtained from their XPS spectra in company with their counterparts from literature [22–23] are given in Table 2. In the entire Pt spectra, the $4f_{7/2}$ signal at around 71.50 eV in all catalysts are assigned to zero-valent Pt. The relatively large shift from the value of 70.9 eV of bulk Pt-metal is attributed to a significant contribution from the metal-support interaction or small cluster-size effects [23]. The comparison with the data from literature suggests that the main part of Pt of the in-house catalysts is in metallic state. The binding energies of Sn are slightly higher than both reference data, due to interactions between Sn and Pt, due to a higher Sn content or due to small cluster-size effects. From these experimental

Table 1
XRD and TEM results of carbon supported Pt and PtSn catalysts

Catalyst	$2\theta_{max}$[a] (°)	Lattice parameter (Å)	$B_{(2\theta)}$[b] (mrad)	Mean particle size (nm)	
				XRD	TEM
Pt/C	67.62	3.9156	64.18	2.6	2.7
1/1	66.24	3.9873	78.88	2.1	2.3
3/2	66.50	3.9735	87.26	1.9	2.2
PtSn/C					
2/1	66.82	3.9562	63.88	2.6	3.0
(Pt/Sn=)					
3/1	66.89	3.9530	87.47	1.9	2.2
4/1	67.17	3.9383	87.60	1.9	2.3

[a] The angular position of Pt(2 2 0) reflection peak.
[b] The full width at half-maximum (FWHM) of the fitted (2 2 0) peak.

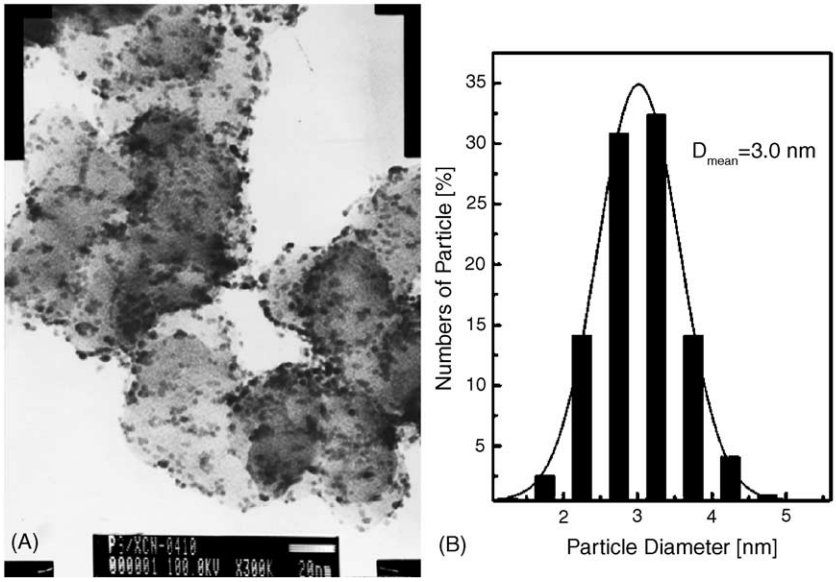

Fig. 1. (A) A typical TEM image of Pt_2Sn_1/C catalyst and (B) the histogram of the PtSn particles size distribution.

results, it is confirmed that the main part of Sn is in oxidized state, although the exact amounts of oxidized Sn and metallic Sn in the catalysts are not defined in the present work.

3.3. Single fuel cell performance results

Carbon supported Pt and PtSn were, respectively used as catalysts and evaluated in the single cell tests as DEFC anodes. The anodes of all single cells employing PtSn as catalysts contain the same platinum loading and different tin loading, which is much cheaper than platinum. The single cells with different anode catalysts show different steady-state polarization curve at 60, 75 and 90 °C, as showed in Figs. 3–5. When Pt/C was used as anode catalyst, the single cell exhibited poor performances at any temperature, even though there was a higher Pt loading (2.0 mg Pt/cm^2) at the anode side.

As seen from Fig. 3 of single cell performance at 60 °C, the cell voltages at a current density lower than 40 mA/cm^2 are increasingly improved as the Sn content in the anode catalysts increases. The single ethanol fuel cell adopting pure Pt as anode catalysts exhibits a very low open-circuit voltage of 0.44 V, which is far from the standard electromotive force of 1.145 V [24]. The great difference between the open-circuit potential and the standard electromotive force is mainly attributed to the lower anode catalytic activity and the ethanol crossover. The ethanol crossover effect is identical in every case of the present work because of the same electrolyte and MEAs preparation procedure used in all single cell tests. The maximum power density of this ethanol fuel cell

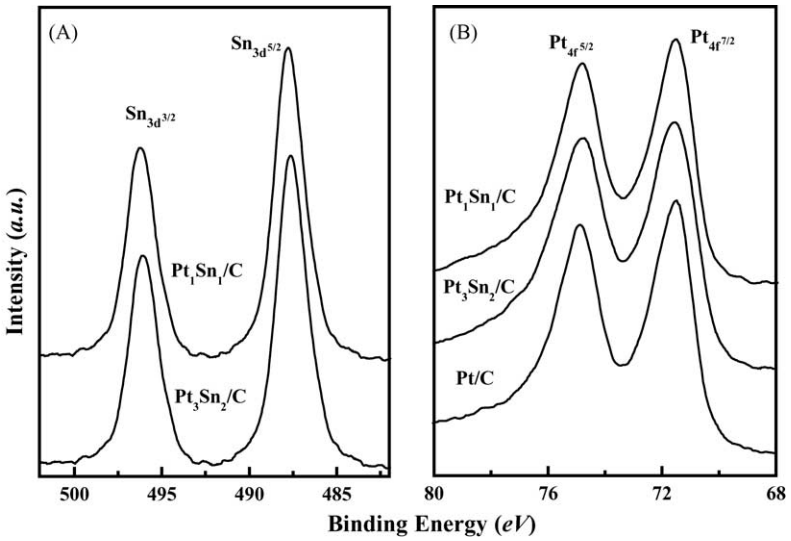

Fig. 2. X-photoelectron spectra of Sn_{3d} and Pt_{4f} for Pt/C, Pt_3Sn_2/C and Pt_1Sn_1/C catalysts.

Table 2
Comparison of binding energies of $Pt_{4f}^{7/2}$ and $Sn_{3d}^{5/2}$ between literature and experiment

References	Data in literature			Experimental data		
	PtO_2	PtO	Pt	Pt/C	Pt_3Sn_2/C	Pt_1Sn_1/C
$Pt_{4f}^{7/2}$						
[22]	74.5	73.6	70.9	71.50	72.03	71.53
[23]	74.5	72.93	71.55			
	SnO_2	Sn		Pt_3Sn_2/C	Pt_1Sn_1/C	
$Sn_{3d}^{5/2}$						
[22]	486.4	484.6		487.60	487.00	
[23]	486.87–487.10[a]	485.26–485.65[a]				

[a] This data changes slightly because of the contents of Sn and total metal loadings.

is only 5.2 mW/cm^2 at the current density of 38.4 mA/cm^2 at 60 °C. When employing Pt_4Sn_1 as anode, the performance of the single ethanol fuel cell is obviously improved in comparison with the single cell with Pt as anode. The open-circuit voltage is increased from 0.44 V (for Pt) to 0.65 V (for Pt_4Sn_1), and the maximum power density is also increased to 15.2 mW/cm^2 at 65.6 mA/cm^2 (Pt_4Sn_1). It is worth noting that the anode Pt loading is 2.0 mg/cm^2 when Pt is used as anode catalyst, while the Pt loading is only 1.3 mg/cm^2 when Pt_4Sn_1 is employed. The total metal loading at the anode for Pt_4Sn_1 is only 1.5 mg (Pt + Sn)/cm^2. As the Sn atomic content of the anode catalysts is increased from 20% (Pt_4Sn_1) to 25% (Pt_3Sn_1), the performance of the single ethanol fuel cell is improved further. The open-circuit voltage increases by about 0.1 V and the maximum power density increases to 23.0 mW/cm^2 at 75.6 mA/cm^2. As the Sn content is increased further, both the open-circuit voltage and the maximum power density of the single ethanol fuel cell are enhanced. However, the differences among the Pt_2Sn_1, Pt_3Sn_2 and Pt_1Sn_1 are not so obvious as those among Pt_3Sn_1, Pt_4Sn_1 and Pt. Although at 60 °C the single ethanol fuel cell with Pt_3Sn_2 as anode catalyst shows the highest maximum power density (30.3 mW/cm^2 at 94.4 mA/cm^2), the single cell with Pt_1Sn_1 shows a better performance in low current density region. The relation between the single ethanol fuel cell performances (the cell power density at a defined current density) at 60 °C and the Sn atomic content in the corresponding anode catalysts is presented in Fig. 3(C). As it can be distinguished from Fig. 3(C), the power densities at 30 and 40 mA/cm^2 increase with the Sn atomic content increment. In terms of the maximum power density, the Pt_3Sn_2 (with Sn content of 40.0 at.%) is more suitable for the single ethanol fuel cell operated at 60 °C.

When the operating temperature is increased to 75 °C, the single ethanol cells with different anode catalysts show improved performances (Fig. 4). Both the open-circuit voltages and the maximum power densities are enhanced in comparison with those obtained at 60 °C. In the current density region from 0 to 80 mA/cm^2, the performances of the single ethanol fuel cells with Pt_1Sn_1, Pt_3Sn_2 and Pt_2Sn_1 are very similar, all of which are better than that of Pt_3Sn_1, Pt_4Sn_1 and Pt, just as both curves in Fig. 4(C) (the lines of 30 and 60 mA/cm^2) show. The single cells employing Pt_3Sn_2 and Pt_2Sn_1 as anode catalysts give the highest maximum power densities of about 40.0 mW/cm^2 at about 105 mA/cm^2. Pt_3Sn_2 and Pt_2Sn_1 are thought as more suitable anode catalysts for direct ethanol fuel cell operated at 75 °C in terms of the maximum power density.

As presented in Fig. 5, at 90 °C, when pure Pt is used as the anode catalyst, a low open-circuit potential of 0.55 V was observed for direct ethanol fuel cell. A significant potential drop of about 0.28 V, more than half of the open-circuit potential, was observed when a current density of 30 mA/cm^2 was passed through the cell, and the corresponding power density at 30 mA/cm^2 was only 8.1 mW/cm^2. This behavior indicates a strong activation control at low current densities, typical of the ethanol-oxidation reaction. The maximum power density of this single cell with Pt/C was only 10.8 mW/cm^2 at 75 mA/cm^2.

From Fig. 5 it can also be seen that the open-circuit voltages of all single cells with PtSn as anode catalyst are above 0.7 V at 90 °C. Both the performances of single cells with Pt_4Sn_1/C and Pt_3Sn_1/C, respectively are inferior to that of the cell employing Pt_1Sn_1/C, but still superior to those employing Pt/C and Pt_1Ru_1/C [25]. The maximum power densities with Pt_4Sn_1/C and Pt_3Sn_1/C are 34.6 and 43.0 mW/cm^2, respectively at about 130 mA/cm^2 at 90 °C. The open-circuit voltage of the cell adopting Pt_2Sn_1/C is 0.81 V, as high as that of the cell with Pt_1Sn_1/C. The cell voltage loss was only 0.13 V as the current density was increased from 0 to 30 mA/cm^2, and the corresponding power density was 20.4 mW/cm^2 at 30 mA/cm^2. The cell voltage decreased quite slowly from 0.68 V (at 30 mA/cm^2) to 0.61 V (at 60 mA/cm^2). The maximum power density of this cell reached 61.2 mW/cm^2 at the current density of 146 mA/cm^2, after which there is a drop of cell voltage as the current density increases. When the Sn atomic content increases to 40%, namely when Pt_3Sn_2/C is employed as the anode catalyst, the open-circuit voltage is up to 0.82 V. The cell voltages are 0.68 and 0.59 V at 30 and 60 mA/cm^2, respectively. The peak power density is 55.8 mW/cm^2 at the corresponding current density of 135.6 mA/cm^2. As Pt_1Sn_1/C was employed as the anode catalyst, the open-circuit voltage of single cell rises to 0.81 V compared to 0.55 V of single cell with Pt/C. There is a small

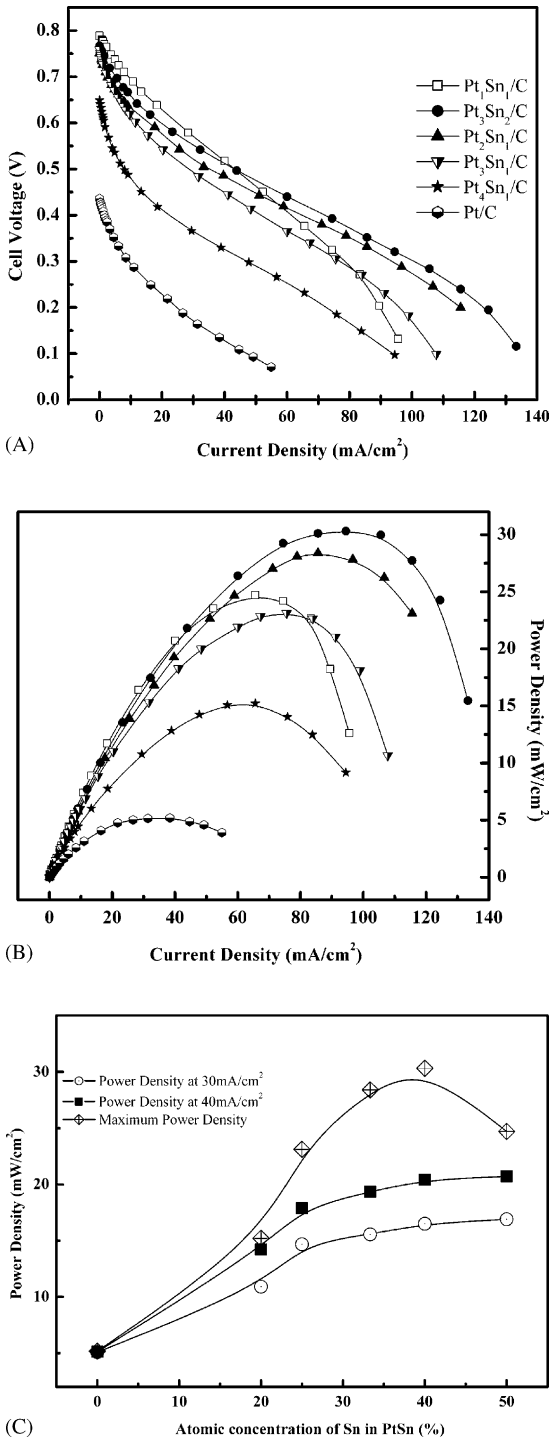

Fig. 3. Performance comparison of PtSn anode based direct ethanol fuel cells at 60 °C. Anode catalyst: carbon supported PtSn with different Pt/Sn atomic ratio with a Pt loading of 1.3 mg/cm^2, $C_{ethanol}$ = 1.0 mol/L, flow rate: 1.0 mL/min. Cathode: (20 Pt wt.%, Johnson Matthey Corp.) with a loading of 1.0 mg Pt/cm^2, P_{O_2} = 2 bar. Electrolyte: Nafion®-115 membrane.

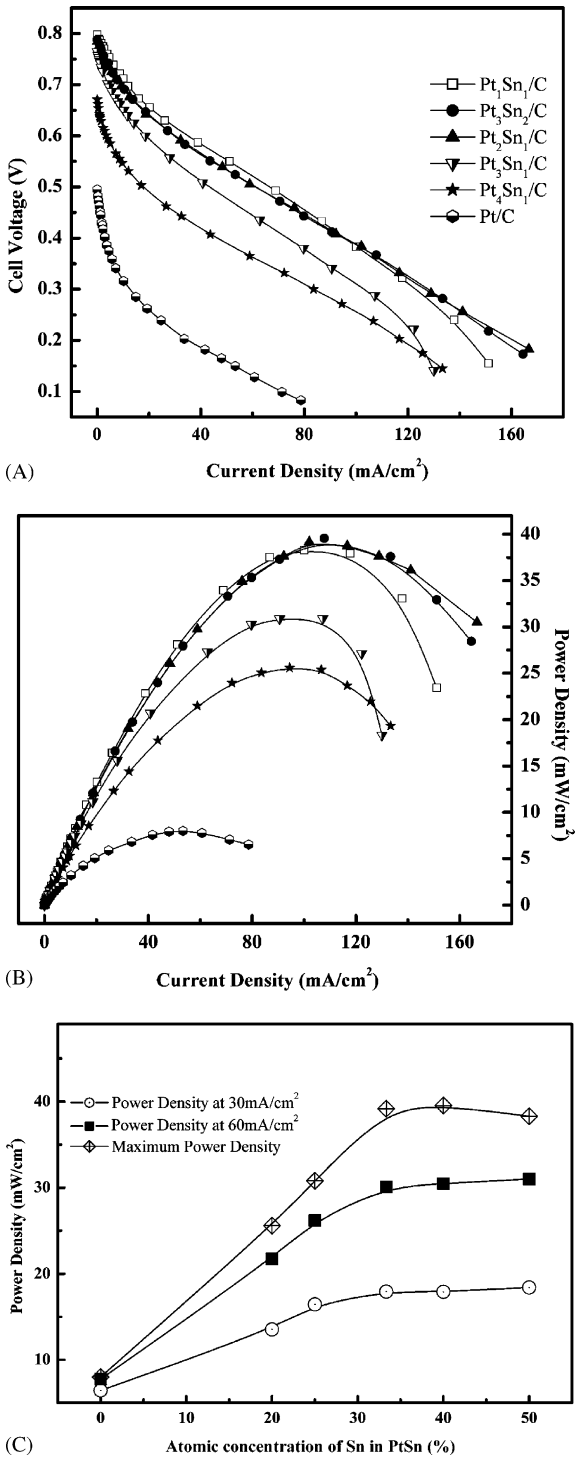

Fig. 4. Performance comparison of PtSn anode based direct ethanol fuel cells at 75 °C. Anode catalysts: carbon supported PtSn with different Pt/Sn atomic ratio with a Pt loading of 1.3 mg/cm^2, $C_{ethanol}$ = 1.0 mol/L, flow rate: 1.0 mL/min. Cathode: (20 Pt wt.%, Johnson Matthey Corp.) with a loading of 1.0 mg Pt/cm^2, P_{O_2} = 2 bar. Electrolyte: Nafion®-115 membrane.

voltage drop of about 0.15 V when the current density increases from 0 to 30 mA/cm^2 in the activation-control region. The cell voltage with Pt_1Sn_1/C at 30 mA/cm^2 is comparable to the open-circuit voltage of the single ethanol cell with Pt_1Ru_1/C [25], which indicates that Pt_1Sn_1/C is more active to ethanol electro-oxidation than Pt_1Ru_1/C, which is primarily used as anode catalysts for methanol electro-oxidation and CO-tolerance at present. Even at the current density of

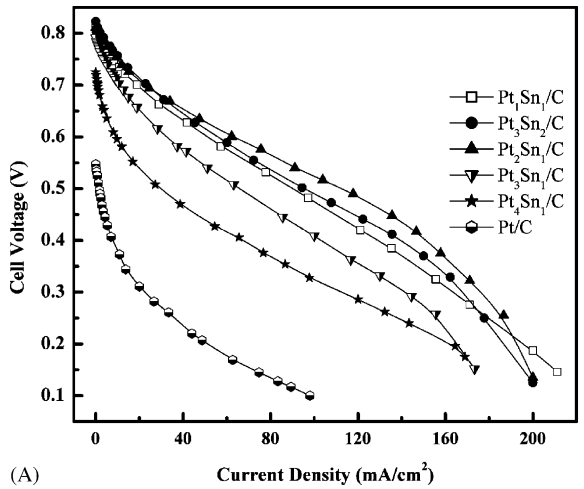

(A)

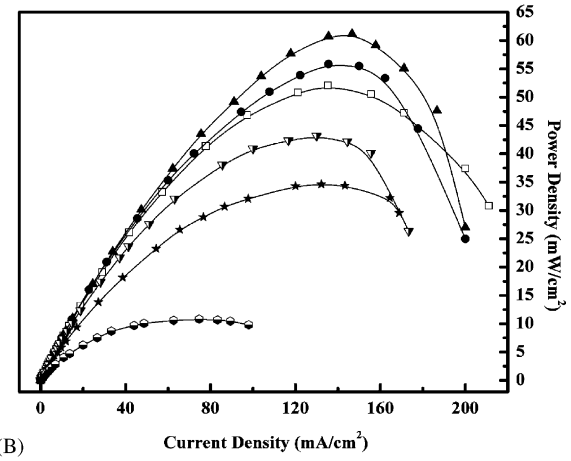

(B)

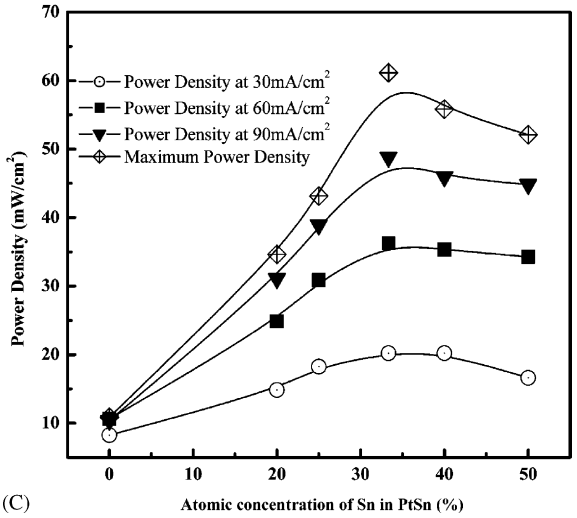

(C)

Fig. 5. Performance comparison of PtSn anode based direct ethanol fuel cells at 90 °C. Anode catalysts: carbon supported PtSn with different Pt/Sn atomic ratio with a Pt loading of 1.3 mg/cm^2, $C_{ethanol}$ = 1.0 mol/L, flow rate: 1.0 mL/min. Cathode: (20 Pt wt.%, Johnson Matthey Corp.) with a loading of 1.0 mg Pt/cm^2, P_{O_2} = 2 bar. Electrolyte: Nafion®-115 membrane.

60 mA/cm^2, the cell voltage is still as high as 0.58 V, and the corresponding power density is 34.8 mW/cm^2, still higher than the maximum power density of the single cell with Pt_1Ru_1/C. The cell voltage decreases to 0.5 V as the current density increases to 90 mA/cm^2, with a corresponding power density of 45.0 mW/cm^2. This single cell gives a peak power density of 52.0 mW/cm^2, nearly five times that of the single cell with Pt/C. The performances of the single cells with different PtSn catalysts at 90 °C are shown in Fig. 5(C). It is clear that there is a power density peak in each performance curve at the same Sn atomic content of about 33%, and the corresponding Pt/Sn atomic ratio is 2. From the practical point of view, the single cell test is the final evaluation criterion for a novel electrocatalyst and electrolyte, although there are so many factors affecting the performance of a single cell such as the MEA fabrication and the activities and conductivities of the electrocatalysts. In the present work, the anode catalyst is the one and only variable and other factors such as cathode catalyst, electrolyte and MEA preparation parameters are defined. Therefore, the single cell performances with different anode catalysts can be used to compare the activities of anode catalysts to a certain extent.

For the sake of comparison, PtRu/C prepared by the similar method to PtSn/C, with almost the same average particle size, was also used as the ethanol anode oxidation electrocatalysts [19]. As one can see from Fig. 6 of the anode polarization results of different anode catalysts, the Pt_2Sn_1 catalyst demonstrates higher activity to ethanol electro-oxidation than Pt_3Sn_2 in the potential region lower than 350 mV (versus DHE). From this figure, it is also clear that both Pt_2Sn_1 and Pt_3Sn_2 are more active than PtRu for ethanol electro-oxidation. The polarization test is in accordance with the results of single fuel cell test, both of which indicate that anode activities and consequently single fuel cell performances are different from each other with different anode catalysts and current densities.

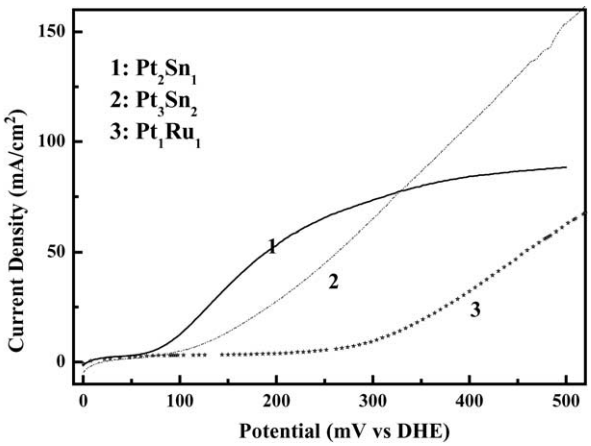

Fig. 6. Anode polarization results of ethanol on carbon supported Pt_1Sn_1, Pt_3Sn_2 and Pt_1Ru_1 catalysts at 90 °C. Anode metal loading: 1.3 mg Pt/cm^2. Ethanol concentration and flow rate: 1.0 mol/L ethanol and 1.0 mL/min. Nafion®-115 was the electrolyte. Counter and reference electrode: Pt/C (20%, 1.0 mg Pt/cm^2). Scan rate was 2 mV/s.

The activity of anode catalysts to ethanol electro-oxidation is affected by catalyst surface structure, metallic particle size, the interaction between active components and other factors. In the present work, the metallic particle size effect on the ethanol electro-oxidation is not excluded, although it was not verified at present. On the other hand, all the catalysts synthesized with the same method had similar particle size, thus there might be almost the same particle size effects if they exist. Furthermore, Sn or its oxides, as well as Ru, can supply surface oxygen-containing species for the oxidative removal of CO-like species strongly adsorbed on adjacent Pt active sites, which is the so-called bi-functional mechanism [17,26,27], and activate the chemisorbed CO-like intermediates [28,29]. Thus, the addition of Sn to Pt enhances the ethanol electro-oxidation activity, and consequently improves the fuel cell performance compared to the cell with pure Pt/C as anode catalysts. One of the noticeable differences among these catalysts is the change in lattice parameters characterized from the XRD results as mentioned above. Ethanol electro-oxidation is different from methanol electro-oxidation in that the former involves the cleavage of the C–C bond besides the oxidative removal of the poisoning species such as CO_{ads}. A possible explanation is that the extended lattice parameter favors the cleavage of the C–C bond, improving the fuel utilization and consequently the performance of the fuel cell. Therefore, PtSn catalysts not only promote the cleavage of C–C bond but also improve the removal of CO_{ads} species [17] formed on the platinum surface during ethanol electro-oxidation, and consequently enhance the ethanol electro-oxidation. It is suggested that the higher content of Sn oxide due to the fact that Sn is increased could lead to a decrement of the anode electronic conductivity because of the poor electronic conductivity of tin oxide. This could result in an increment of the internal resistance of the fuel cell, deteriorating the cell performance and counteracting to a certain extent the promotion effect of Sn on Pt electrocatalytic activity to ethanol electro-oxidation. On the other hand, Pt active sites of catalysts with a high Sn content could be partly blocked by surface Sn or its oxides, which will inhibit ethanol adsorption when ethanol adsorption is the rate-determining step at high current density or at higher temperatures. These opposite effects mentioned above and the operation conditions determine the optimum content of Sn for DEFC.

Given the factors mentioned above and evaluated from the present results, Pt_3Sn_2/C is a more suitable anode catalyst for the direct ethanol fuel cell at 60 °C. The direct ethanol fuel cells employing Pt_2Sn_1/C and Pt_3Sn_2/C have the similar performance at 75 °C. At 90 °C Pt_2Sn_1/C is demonstrated to be a more suitable anode catalyst for direct ethanol fuel cells.

Acknowledgements

The authors would like to thank the “Greece-China Joint Research and Technology Programme 2003–2005” and the National Natural Science Foundation of China (Grant No.: 20173060) for funding.

References

[1] J. Zhang, K.M. Colbow, D.P. Wilkinson, US Patent 6,187,467 (2001).
[2] X. Ren, P. Zelenay, S. Thomas, J. Davey, S. Gottesfeld, J. Power Sources 86 (2000) 111.
[3] H. Chang, J.R. Kim, J.H. Cho, H.K. Kim, K.H. Choi, Solid State Ion 148 (2002) 601.
[4] M.M. Mench, Z.H. Wang, K. Bhatia, C.Y. Wang, in: Proceedings of the International Mechanical Engineering Congress and Exposition (IMECE), 11–16 November 2001.
[5] D. Buttin, M. Dupont, M. Straumann, R. Gille, J.C. Dubois, R. Ornelas, G.P. Fleba, E. Ramunni, V. Antonucci, A.S. Aricò, P. Creti, E. Modica, M. Pham-Thi, J.P. Ganne, J. Appl. Electrochem. 31 (2001) 275.
[6] P.J. Sebastian, J. New Mat. Electrochem. Syst. 4 (2001) 1.
[7] S.C. Thomas, X.M. Ren, S. Gottsfeld, P. Zelenay, Electrochim. Acta 47 (2002) 3741.
[8] H. Dohle, H. Schmitz, T. Bewer, J. Mergel, D. Stolten, J. Power Sources 106 (2002) 313.
[9] W. Li, W. Zhou, H. Li, Z. Zhou, B. Zhou, G. Sun, Q. Xin, Electrochim. Acta 49 (2004) 1045.
[10] K.-W. Park, J.-H. Choi, S.-A. Lee, C. Pak, H. Chang, Y.-E. Sung, J. Catal. 224 (2004) 236.
[11] L. Dubau, F. Hahn, C. Coutanceau, J.-M. Léger, C. Lamy, J. Electroanal. Chem. 554/555 (2003) 407.
[12] M.-S. Löffler, H. Natter, R. Hempelmann, K. Wippermann, Electrochim. Acta 48 (2003) 3047.
[13] E.V. Spinacé, A.O. Neto, M. Linardi, J. Power Sources 129 (2004) 121.
[14] A. Oliveira Neto, E.G. Franco, E. Aricó, M. Linardi, E.R. Gonzalez, J. Eur. Ceram. Soc. 23 (2003) 2987.
[15] C. Lamy, S. Rousseau, E.M. Belgsir, C. Coutanceau, J.-M. Léger, Electrochim. Acta 49 (2004) 3901.
[16] W. Zhou, W. Li, S. Song, Z. Zhou, L. Jiang, G. Sun, Q. Xin, K. Poulianitis, S. Kontou, P. Tsiakaras, J. Power Sources 131 (2004) 217.
[17] F. Delime, J.-M. Léger, C. Lamy, J. Appl. Electrochem. 29 (1999) 1249.
[18] R. Ianniello, V.M. Schmidt, J.L. Rodriguez, E. Pastor, J. Ealactroanal. Chem. 471 (1999) 267.
[19] W.J. Zhou, Z.H. Zhou, S. Song, W. Li, G.Q. Sun, P. Tsiakaras, Q. Xin, Appl. Catal. B 46 (2003) 273.
[20] V. Radmilović, H.A. Gasteiger, P.N. Ross, J. Catal. 154 (1995) 98.
[21] Z.B. Wei, S.L. Wang, B.L. Yi, J.G. Liu, L.K. Chen, W.J. Zhou, W.Z. Li, Q. Xin, J. Power Sources 1/2 (2002) 364.
[22] C.D. Wagner, W.M. Riggs, L.E. Davis, J.F. Moulder, G.E. Muilenberg, Handbook of X-ray Photoelectron Spectroscopy, Perkin-Elmer Corp., 1979.
[23] A.K. Shukla, A.S. Aricò, K.M.E. Khatib, H. Kim, P.L. Antonucci, V. Antonucci, Appl. Surf. Sci. 137 (1999) 20.
[24] C. Lamy, E.M. Belgsir, J.-M. Leger, J. Appl. Electrochem. 31 (2001) 799.
[25] W.J. Zhou, Z.H. Zhou, W.Z. Li, S.Q. Song, G.Q. Sun, Q. Xin, D. Sarantarides, K. Poulianites, P. Tsiakaras, Proceedings of the Eigth Grove Fuel Cell Symposium, ExCel, London, UK, 24–26 September 2003.
[26] B. Gurau, R. Viswanathan, R. Liu, T.J. Lafrenz, K.L. Ley, E.S. Smotkin, E. Reddington, A. Sapienza, B.C. Chan, T.E. Mallouk, S. Sarangapani, J. Phys. Chem. B. 102 (1998) 9997.

[27] T.E. Shubina, M.T.M. Koper, Electrochim. Acta 47 (2002) 3621.
[28] J.L. Margitfalvi, I. Borbáth, M. Hegadűs, Á. Szegedi, Catal. Today 73 (2002) 343.
[29] Y. Morimoto, E.B. Yeager, J. Electroanal. Chem. 441 (1998) 78;
Y. Morimoto, E.B. Yeager, J. Electroanal. Chem. 444 (1998) 95.